Chapter 1

Surface Modification of Polyimide Films for Inkjet-Printing of Flexible Electronic Devices

Yunnan Fang and Manos M. Tentzeris

Additional information is available at the end of the chapter

http://dx.doi.org/10.5772/intechopen.76450

Abstract

Kapton polyimide films are one of the most commonly used flexible and robust substrates for flexible electronic devices due to their excellent thermal, chemical, mechanical, and electrical properties. However, such films feature an inert and highly hydrophobic surface that inhibits the deposition of functional materials with water-based fluids (solutions, suspensions, inkjet inks, *etc*.), which raise the need for their surface modification to reduce their inherent surface inertness and/or hydrophobicity in order to allow for the fabrication of electronic devices on the substrates. Traditional Kapton surface modification approaches use harsh conditions that not only cause environmental and safety problems but also compromise the structural integrity and the properties of the substrates. This chapter focuses on two recently-developed mild and environmentally friendly wet chemical approaches for surface modification of Kapton HN films. Unlike the traditional methods that target the polyimide matrix of Kapton films, these two methods target the slip additive embedded in the polyimide matrix. The surface modified Kapton films resulted from these two methods allowed for not only great printability of both water- and organic solvent-based inks (thus facilitating the full-inkjet-printing of entire flexible electronic devices) but also strong adhesion between the inkjet-printed traces and the substrate films.

Keywords: surface modification, Kapton, polyimide, flexible electronic devices, sensors, inkjet-printing

1. Introduction

Kapton HN films, which are well known to be made of polyimide polymer, are one of the most commonly used substrates for flexible electronics due to their excellent physical and

electrical properties as well as exceptional thermal and chemical stability. However, such films feature an inert and highly hydrophobic surface. Hydrophilic (e.g. water-based) fluids (solutions, suspensions, inks, *etc*.) will ball up on such surfaces (due to "lotus effect") [1, 2]. However, for fabrication of an entire electronic device, both organic solvent- and water-based fluids are usually needed to deposit functional materials on the same substrate surface. As a result, surface modifying polyimide substrates to reduce their inherent surface hydrophobicity and/or inertness is usually needed to allow for the continuous and uniform deposition with both organic solvent- and water-based fluids.

Traditionally, polyimide substrates are surface modified with a number of methods including plasma [3, 4] and ion-beam [5, 6] etching, UV/ozone exposure [3, 7], acid [3, 8] and/or base [9, 10] treatments, and laser ablation [11, 12]. These methods, however, usually compromise the structural integrity and the properties (such as the cohesive strength, and the thermal and chemical stability) of the polyimide substrate, since they utilize relatively harsh conditions to oxidize and/or tear out part of the surface polyimide. Additionally, the wastes and by-products (such as acrolein which is extremely irritating, strong bases and acids which are corrosive, and benzene which is carcinogenic) generated from these harsh treatments can raise serious environmental and safety issues (especially when the treatments are performed indoors and/or in large scales). For example, incubation with a sodium hydroxide solution has been one of the most common traditional methods to tune the surface properties of Kapton polyimide substrates [9, 10, 13], but such a treatment not only generates highly corrosive strong base waste but also tears out some surface polyimide resulting in pits in the Kapton surface [14]. The defects on structurally damaged Kapton films would result in not only poor deposition quality of the device components but also weakened mechanic strength of the resulting devices. The increasingly growing of flexible electronic devices (such as flexible displays [15], electronic paper [16, 17], photovoltaic cells [18, 19], sensors [1, 2, 20–23], LEDs [24], electronic textiles [25], RF tags [26], and electrochemical devices [27], *etc*.) is calling for mild and environmentally friendly surface modification approaches which can minimize the compromise to the structural integrity and the properties of Kapton polyimide substrates while efficiently tuning the surface properties of the substrates. To take full advantage of the properties of Kapton HN films, any surface modification to such films should avoid as much as possible compromising their structural integrity and properties. For extremely thin Kapton HN films, such as Kapton 30HN (thickness 7.5 μm), 50HN (thickness 12.7 μm), and 75HN (thickness 19.1 μm), it is critical to make sure that their surface modification is non- or minimally destructive.

Kapton HN films have a slip additive incorporated in the polyimide matrix to enhance their mechanical properties [13]. The nature of the additive, however, has been very scarcely reported in the literature. Williams *et al.* has mentioned, but without providing supporting data, that the additive in Kapton HN films was calcium phosphate dibasic ($CaHPO_4$) [14]. This chapter first describes the characterization of Kapton 500HN films particularly of their slip additive, then introduces two recently-developed mild and environmentally friendly wet chemical approaches for surface modification of Kapton HN films to allow for not only great printability of both water- and organic solvent-based inks but also strong adhesion between the inkjet-printed traces and the surface modified substrates. Unlike the aforementioned traditional Kapton surface modification methods which target, and oxidize and/or tear out part of, the surface polyimide matrix, the approaches described in this chapter target the electric charges on the slip additive particles.

2. Characterization of Kapton HN films

In this section, a number of characterizations were performed on as-received Kapton 500HN films (a gift from Dupont, Wilmington, DE, USA) particularly on their slip additive. The optical microscopy analysis of the films showed particles of varying sizes which were imbedded in Kapton HN polyimide matrix (**Figure 1a**). These particles have been shown to be the slip additive to the polyimide matrix of Kapton HN [14, 28]. As shown in **Figure 1a**, the majority of the slip additive particles exuded to the substrate surface, which is consistent with a previous observation [29]. The large hump (with 2θ ranging from ~10° to ~35°) and the sharp narrow peaks in the X-ray diffraction (XRD) pattern of the Kapton HN films (**Figure 1b**) indicated the presence of amorphous and crystalline components, respectively. Apparently the amorphous moiety was the polyimide polymer and crystalline moiety the slip additive. While calcium phosphate dibasic ($CaHPO_4$) might be present in the additive as previously reported [14], the crystalline peaks in the XRD pattern of the Kapton HN films matched very well with those of calcium carbonate ($CaCO_3$) (ICDD reference code 04–001-7249) (**Figure 1b**) but did not match any of the $CaHPO_4$ peaks. Significant carbon and oxygen peaks and a small calcium peak showed up in the energy dispersive X-ray spectroscopy (EDX) pattern of the Kapton substrate (**Figure 1c**).

To better characterize the slip additive in Kapton HN films, efforts were made to minimize the interference from the polyimide polymer matrix. Kapton HN films were fired at 800°C for 2 hours in air (this firing treatment has been shown to be efficient to pyrolyze the entire polyimide polymer moiety in Kapton HN [30]) to remove the polyimide polymer. The remaining inorganic components were characterized with scanning electron microscopy (SEM), EDX, and XRD analyses.

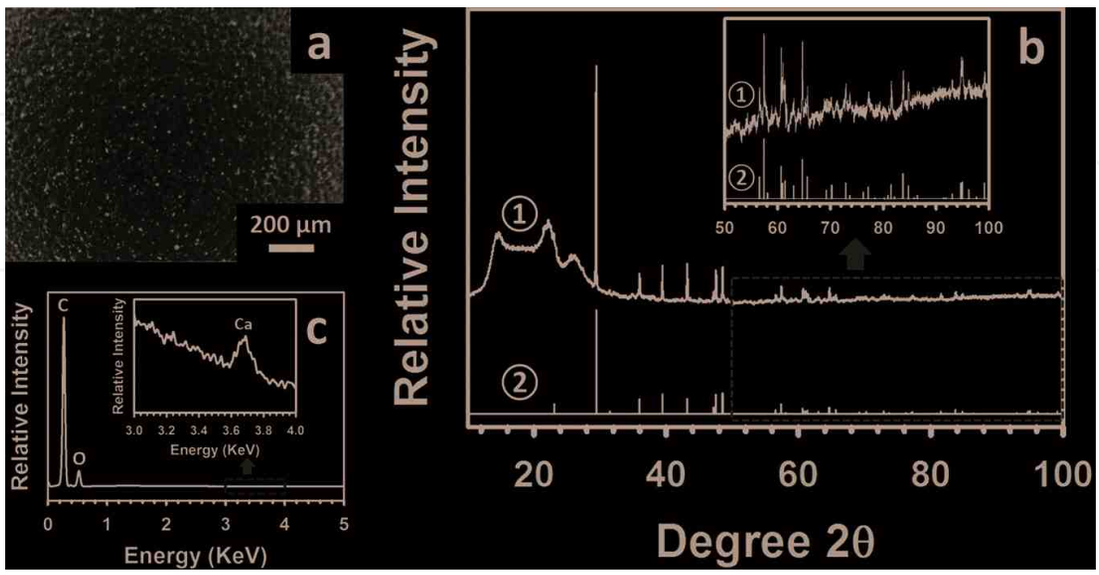

Figure 1. Kapton HN film characterization. (a) Optical microscopy analysis of a blank Kapton HN film. (b) XRD analysis of the specimen shown in (a) (pattern ①) and reference $CaCO_3$ (pattern ②, ICDD reference code 04–001-7249) (inset: Locally enlarged XRD pattern to show the area with a 2θ of from 50° to 100°). (c) EDX analysis of the specimen shown in (a) (inset: Locally enlarged EDX pattern to show the calcium peak) [2] (licensed under creative commons attribution 4.0 international license).

As shown in **Figure 2a** and **b**, the size of the ash particles varied significantly, from less than 100 nm to several microns, with the large particles probably resulting from the sintering and agglomeration of the fine ones [14]. The EDX analysis of the ash showed the presence of the elements of oxygen, calcium, and phosphorus (**Figure 2c**). The XRD analysis of the ash showed the presence of only calcium pyrophosphate $Ca_2P_2O_7$ (ICDD Reference code 04–009-6231) (**Figure 2d**). Compared with the XRD pattern of the as-received Kapton HN films (**Figure 1b**), the XRD pattern of the pyrolyzed films (**Figure 2d**) indicated the disappearance of $CaCO_3$ and the presence of $Ca_2P_2O_7$. The composition change was due to the multiple chemical reactions (such as the decomposition of $CaCO_3$ into CaO and CO_2 [31]) taken place during the pyrolyzing process. Combining **Figure 1** (characterization of Kapton HN) and **Figure 2** (characterization of the Kapton HN ash resulted from pyrolysis), we can conclude that the additive in Kapton HN was composed of $CaCO_3$ (crystalline) and one or more phosphorus-containing compounds (crystalline or amorphous). Any calcium phosphate compounds, if present as previously reported [14] in the additive, must be either crystalline but in a small amount (i.e. beyond the detection limit of the diffractometer used for the XRD analyses) or amorphous, or both. While the exact nature of the additive in Kapton HN is probably proprietary

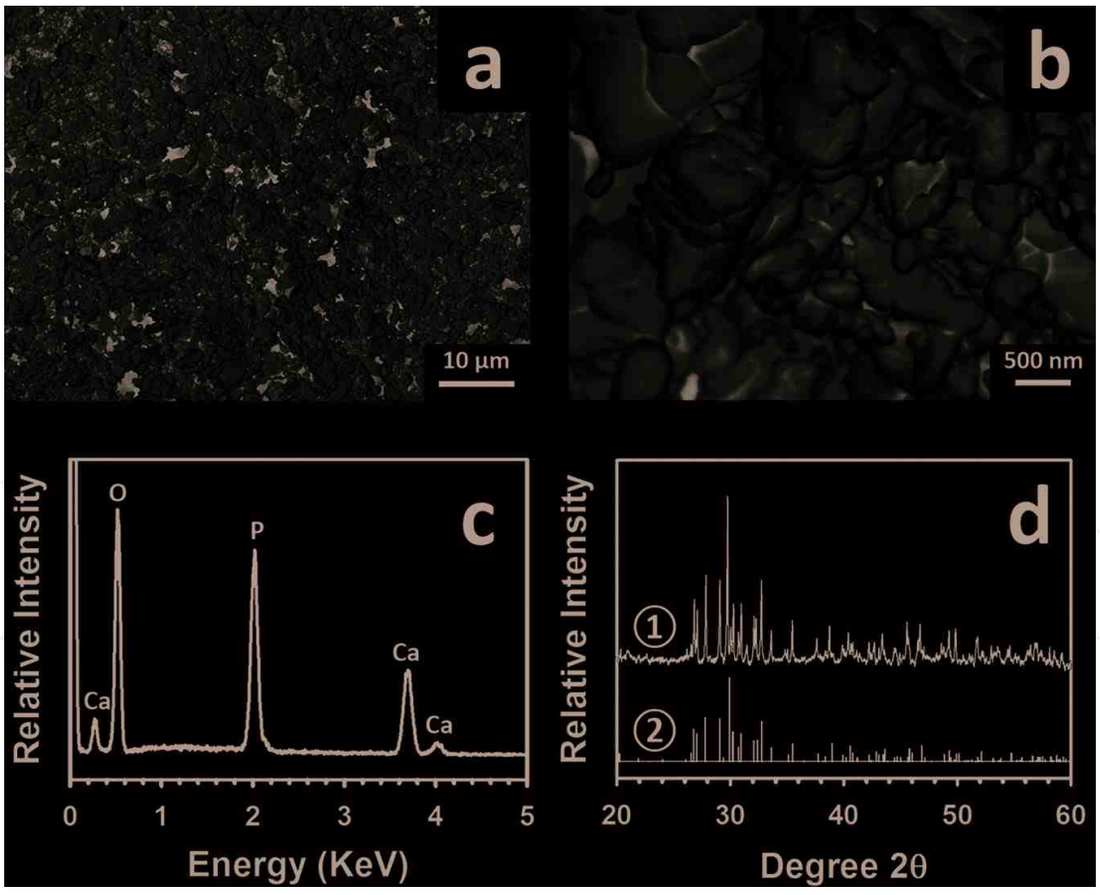

Figure 2. Characterization of the Kapton HN ash resulted from the pyrolysis of Kapton HN films at 800°C for 2 hours in air. (a) and (b) SEM images of the ash with low (a) and high (b) magnifications. (c) EDX pattern of the ash. (d) XRD patterns of both the ash (pattern ①) and reference calcium pyrophosphate $Ca_2P_2O_7$ (pattern ②. ICDD reference code 04–009-6231) [2] (licensed under creative commons attribution 4.0 international license).

and unknown to the public, XRD analyses showed that crystalline $CaCO_3$ was present in the additive in a significant amount (**Figure 1b**). With an isoelectric point of 8.2 [32], crystalline $CaCO_3$ bears positive charges at a neutral or acidic pH. The two recently developed mild and environmentally friendly wet chemical approaches described below both target the surface electric charges borne by the additive particles imbedded in the polyimide matrix of Kapton HN films.

3. A bio-enabled maximally mild layer-by-layer Kapton surface modification approach

Protamine has been clinically used to reverse the anticoagulant effects of heparin by binding to it [33, 34]. The development of the present bio-enabled surface modification approach was inspired by the *in vivo* antagonizing interaction of these two clinically used biological molecules. In this surface modification process, negatively charged heparin and positively charged protamine were used to uniformly deposit a thin film of protamine-heparin complex on Kapton HN substrates in a layer-by-layer fashion. The surface modification process was conducted under maximally mild conditions (in aqueous solutions of clinical biomolecules, and at a neutral pH, room temperature and atmospheric pressure). During the process the positively charged additive particles (e.g. $CaCO_3$ particles) on the Kapton HN surface enabled binding of the initial heparin (negatively charged) layer via electrostatic interaction. After the initial binding of heparin, the layer-by-layer uniform deposition of the protamine-heparin complex on Kapton HN was realized by the electrostatic interaction between the oppositely charged protamine and heparin molecules.

As far as we know, the present bio-inspired method was the first to use environmentally friendly clinical biomolecules for substrate surface modification. It is also the first surface modification approach performed under maximally mild and minimally destructive conditions.

3.1. Surface modification of Kapton HN films

A small Kapton piece with appropriate dimensions (e.g., 50 mm × 50 mm) was cut from a Kapton 500HN sheet. After a brief rinse with a phosphate buffer (0.2 M, pH 7.0), the Kapton piece was incubated for 10 min with a heparin sodium solution (10 mg/ml, pH 7.0) in the phosphate buffer followed by rinsing three times with the phosphate buffer. The Kapton piece was then incubated for 10 min with a protamine sulfate solution (10 mg/ml, pH 7.0) in the phosphate buffer followed by rinsing three times with the phosphate buffer. This process (heparin/rinse/protamine/rinse) was performed for a total of 5 times. Finally, the Kapton piece was rinsed with DI water and dried in air at 60°C for 2 hours.

A control surface modification process was conducted to validate the hypothesis that the surface modification process was facilitated by the positive electric charges on the Kapton HN surface. The control process was similar to the standard process described earlier, except that the heparin solution used in each deposition cycle was supplemented with 1 M sodium chloride.

3.2. Printability assessment

Figure 3a and **b** show the optical images with low and high magnifications, respectively, of some proof-of-concept silver interdigitated electrode (IDE) patterns inkjet-printed on a surface-modified Kapton substrate with an ethanediol-based silver nanoparticle ink (Sun Chemical Corporation, Parsippany, NJ, USA), while **Figure 3c** shows the optical image of some proof-of-concept graphene patches inkjet-printed on a surface modified Kapton substrate with a cyclohexanone/terpineol-based graphene ink which had been formulated based on the procedures described by Secor *et al.* [35]. Both the silver (**Figure 3a** and **b**) and the graphene (**Figure 3c**) patterns printed with organic solvent-based inks were very similar to the designs and exhibited accurately controlled shapes with sharp edges.

A number of shapes (rectangle, circle with a 100 μm-wide gap in the center, and diamond) were then printed on both surface unmodified and surface modified Kapton HN films with a home-made water-based graphene oxide (GO) ink. As shown in **Figure 4a–c**, accurately controlled shapes were able to be inkjet-printed as designed on a surface modified Kapton HN film. On the other hand, the GO ink drops balled up and formed isolated small "islands" on a surface unmodified Kapton HN film (**Figure 4d–f**). As shown in **Figure 4g–i**, the GO ink that was printed on the Kapton film which had been treated with the control process (which was similar to the standard process except that the heparin solution used in each deposition cycle was supplemented with 1 M sodium chloride) balled up and exhibited isolated small "islands," similar to the patterns with surface unmodified Kapton HN shown in **Figure 4d–f**. This validated the hypothesis that the present surface modification method was made possible by the electric charges on the Kapton HN surface. Indeed, with such a high concentration of NaCl present in the heparin solution, the Cl^- ions will screen the positive electric charges on the Kapton HN film surface. As a result, the initial heparin binding to the blank substrate film, and the subsequent protamine and heparin binding to the substrate, will all be drastically

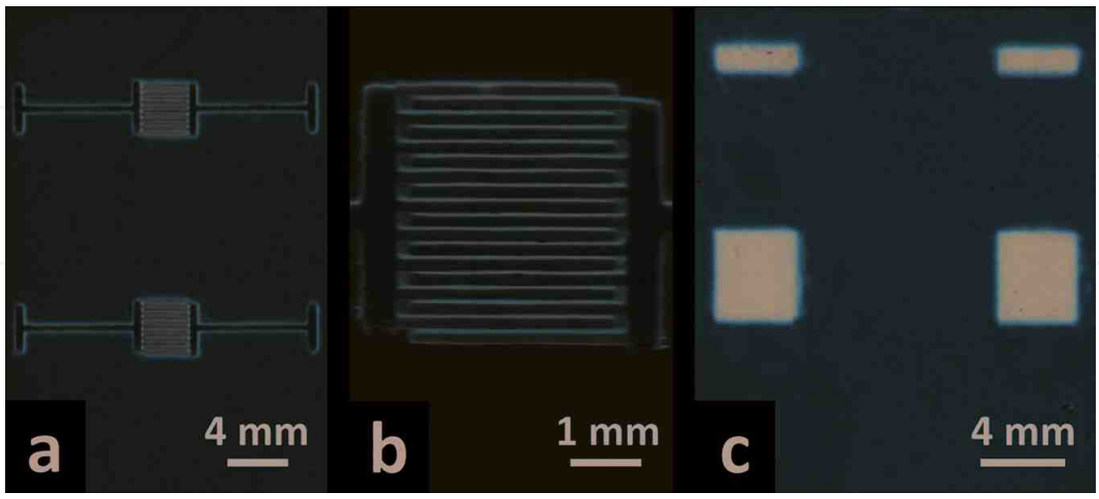

Figure 3. Optical images of proof-of-concept silver IDEs and graphene patches printed on surface modified Kapton HN films with an ethanediol-based silver nanoparticle ink and a cyclohexanone/terpineol-based graphene ink, respectively. (a) and (b) Low (a) and high (b) magnification optical images of the silver IDEs fabricated by printing (for five passes) the silver nanoparticle ink on a surface modified Kapton film followed by annealing at 120°C for 3 hours. (c) Optical image of the graphene patches fabricated by printing (for five passes) the graphene ink on a surface modified Kapton film followed by drying at 100°C for 1 hour [2] (licensed under creative commons attribution 4.0 international license).

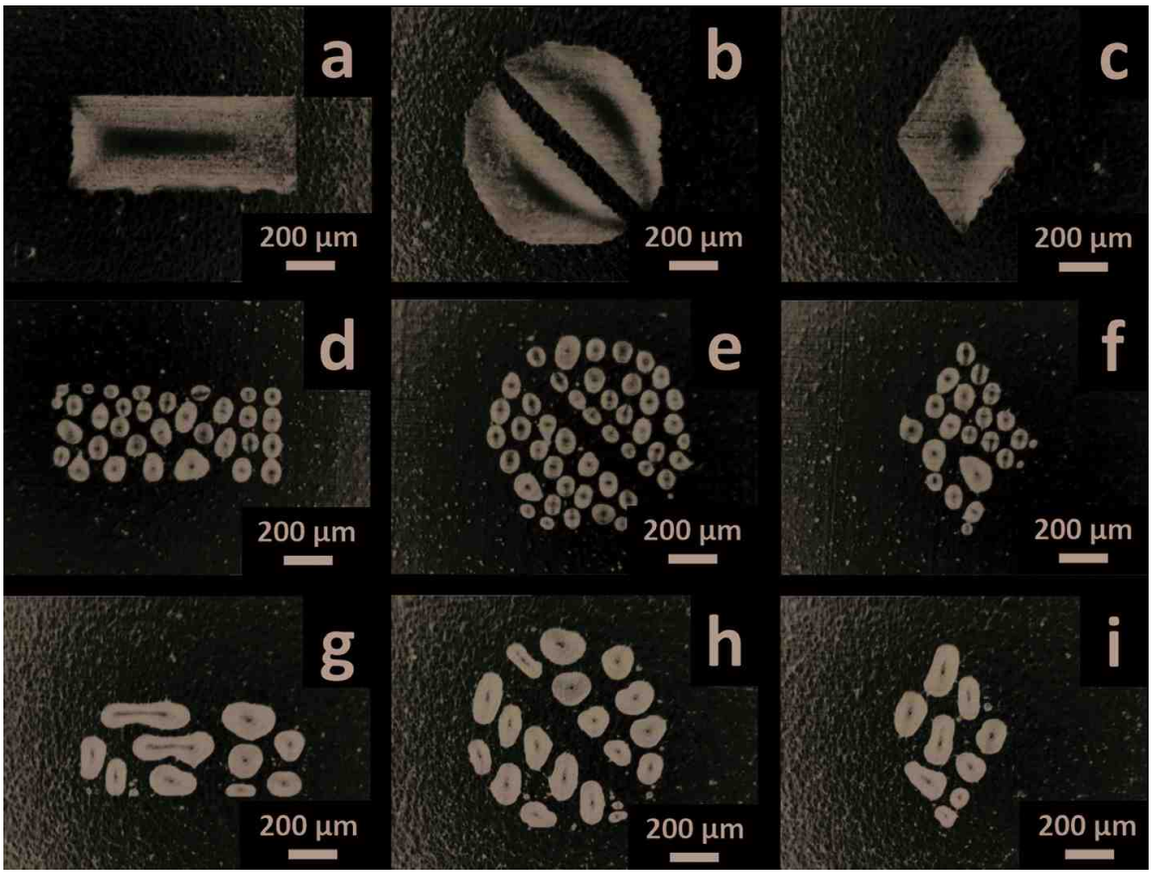

Figure 4. Printability assessment of a water-based GO ink on regularly surface modified (a, b, c), surface unmodified (d, e, f) Kapton HN, and Kapton HN which had been surface modified with a control process which was similar to the regular surface modification process except that 1 M NaCl was supplemented to the heparin solution (g, h, i) [2] (licensed under creative commons attribution 4.0 international license).

reduced. Consequently, the Kapton HN film will not be properly surface modified and its surface properties were hardly tuned.

For ink particles which are electrically charged under particular experimental conditions, the present surface modification method can enhance the uniformity of the thin films deposited on the resulting substrate. This is realized via reduction of "coffee ring effect" during the drying process. In the case of inkjet-printing, "coffee ring effect" results in an appreciable amount of more solid ink material deposited at the substrate perimeter than the other areas upon ink drying. The present surface modification method can choose to terminate the substrate surface with either negatively charged heparin or positively charged protamine. Terminating the substrate surface with opposite electric charges of the ink particles will enable local electrostatic interaction between the substrate surface and the ink particles. Consequently, the migration of the ink particles to the substrate perimeter during drying will be drastically reduced and the uniformity of the inkjet-printed thin films significantly enhanced after drying.

3.3. Fabrication and sensing tests of all-inkjet-printed flexible gas sensors

A flexible multilayered gas sensor was inkjet-printed adhering to the following steps: A Kapton HN film was treated with the process described in the present work, and a water-based

GO ink was then used to inkjet-print a GO patch on the resulting Kapton substrate. The electrically non-conductive GO patch was converted into its conductive reduced graphene oxide (rGO) counterpart by firing at 300°C for 1 hour in nitrogen. A selector layer was inkjet-printed on the resulting rGO patch with a dimethylformamide- (DMF-) based ink containing 10 mg/ml of 2-(2-hydroxy-1, 1, 1, 3, 3, 3-hexafluoropropyl)-1-naphthol. An ethanediol-based silver nanoparticle ink was then used to print two silver electrodes. To achieve an optimum contact between the rGO patch and the silver electrodes, both electrodes overlapped the rGO patch by 1.5 mm. Finally the resulting multi-layered sensor prototype was fired at 120°C for 3 hours to remove the organic molecules coated on the silver nanoparticles and to anneal the silver nanoparticles for desired conductivity. **Figure 5a** shows an optical image of a typical multi-layered gas sensor prototype fabricated with the procedures described above. A flexible single-layered sensor was similarly fabricated except that the selector layer was not printed. Both the multi- and the single-layered sensors were flexible, ultra-lightweight (˜25 mg), and miniature sized (~1.5 cm x 1.0 cm).

Gas sensing was then performed with both multi- and single-layered sensors. A dimethyl methylphosphonate (DMMP) vapor of 2.5 ppm was generated from a DMMP permeation tube (KIN-TEK Laboratories, Inc., La Marque, TX, USA) installed in a FlexStream™ Gas Standards Generator (KIN-TEK Laboratories, Inc.) and carried by nitrogen with a flow rate of 500 sccm. The relative sensitivity of a multi-layered (black solid line) and a single-layered (red-dashed line) sensor upon exposure to 2.5 ppm DMMP is shown in **Figure 5b**. The relative sensitivity (S) is defined by the following formula:

$$S = \frac{R - R_0}{R_0}$$

where R_0 is the resistance between the two silver electrodes of a sensor before the exposure to the DMMP vapor and R that at a particular time after the exposure.

SEM analyses were performed to examine the micro-/nano-morphology of the inkjet-printed GO patterns. A GO patch inkjet-printed (ten passes) on a surface modified Kapton HN film was dried at 95°C under vacuum overnight (to remove the glycerol and the water in the GO ink) and then subjected to SEM analyses. Under a scanning electron microscope, the dried GO

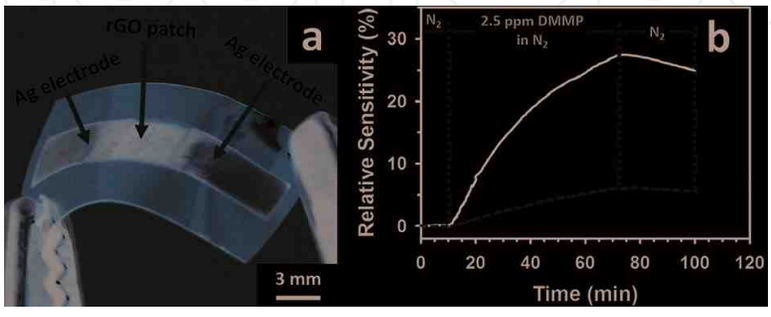

Figure 5. (a) Optical image of a flexible, rGO-based, multi-layered gas sensor inkjet-printed on a surface modified Kapton HN film (the GO ink was printed for 10 passes, the selector ink for one pass, and the silver ink for 5 passes). (b) Relative sensitivity of the multi-layered (black solid line) and the single-layered (red dashed line) gas sensors upon exposure to 2.5 ppm dimethyl methylphosphonate [2] (licensed under creative commons attribution 4.0 international license).

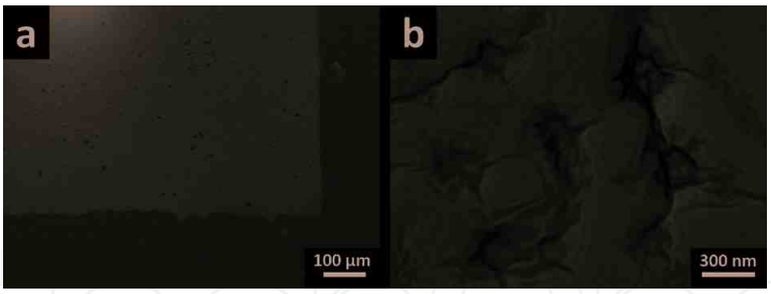

Figure 6. SEM images with low (a) and high (b) magnifications of an inkjet-printed (10 passes) and dried GO film on a surface modified Kapton HN film [2] (licensed under creative commons attribution 4.0 international license).

square had sharp edges as designed and the GO flakes were well interconnected with no observable cracks (**Figure 6a** and **b**).

3.4. Bend cycling tests on an all-inkjet-printed flexible gas sensor

A four-point bend tester (TestResources, Inc., Shakopee, MN, USA) controlled by R Controller software (TestResources, Inc.) was used to conduct the bend cycling tests. A fully inkjet-printed single-layered gas sensor was mounted on the bend tester with a home-made mounting system. The sensor was bent, with an amplitude of 20 mm and a bend rate of 1 mm/second, to a radius of curvature of 1 cm 1000 times in tension and then another 1000 times in compression to the same radius of curvature. After the 2000 bending cycles, the resistance of the sensor was measured with a multimeter and its morphology examined with an optical microscope. It was found that the resistance of the sensor after the bend test was virtually the same as that before the test (i.e. ~14 kΩ) and no morphological changes were observed during the optical analyses. Keeping the amplitude and the bend rate the same, the radius of curvature was reduced to 0.5 cm and the sensor was bent 1000 times in tension and another 1000 times in compression, followed by conductivity and morphology examination. Again, apparent conductivity or morphological changes were not observed.

3.5. Peel testes on an all-inkjet-printed flexible gas sensor

Peel tests were performed via a qualitative Scotch-tape peel test to evaluate the adhesion of an inkjet-printed single-layered gas sensor to the surface modified Kapton film. The adhesive side of a piece of Scotch® magic tape (3 M Company, St. Paul, MN, USA) was firmly pressed against the sensor and then peeled off [36, 37]. By visual inspection and optical microscopic analyses, all three components of the sensor (two silver electrodes and one rGO patch) remained attached to the substrate and retained their intactness after the tape had been peeled off.

4. A computer-controlled polyelectrolyte multilayer-based layer-by-layer Kapton surface modification approach

This is a computer-controlled, facile, environmentally friendly, low-cost, readily scalable, and layer-by-layer deposition process. This process used two weak polyelectrolytes, poly

(acrylic acid) (PAA) and polyethylenimine (PEI), to apply polyelectrolyte multilayers (PEMs) on flexible Kapton HN films in an alternating, layer-by-layer fashion under controlled pH and ionic strength. Compared to strong polyelectrolytes, weak electrolytes have the advantage of controlling the PEM properties more systematically and simply [38]. To our knowledge, this work is the first to use only weak polyelectrolytes to surface modify Kapton substrates.

4.1. Computer-controlled polyelectrolyte multilayer-based surface modification of Kapton HN films

Small pieces of Kapton 500HN with appropriate dimensions (e.g. 95 mm x 95 mm) were cut from a Kapton 500HN sheet and cleaned by sonication, first with a 10 g/L suspension of Powdered Precision Cleaner (Alconox, Inc., White Plains, NY, USA) in DI water for 10 min and then with acetone for 10 min, in an ultrasonic cleaner (Model 2510. Branson Ultrasonics, Danbury, CT, USA). The cleaned Kapton films were rinsed three times with DI water, placed in the sample chamber of a custom-built, computer-controlled, automated deposition system, and then subjected to a layer-by-layer PEM deposition process. The PEM deposition process involved alternating exposure to two solutions of oppositely charged, relatively small polyelectrolyte molecules, polyethylenimine (PEI. Branched, M.W. 1800 Dalton; Alfa Aesar, Ward Hill, MA, USA) and poly (acrylic acid) (PAA. Average M.W. ~1800 Dalton; Sigma-Aldrich, St. Louis, MO, USA). In a typical deposition cycle, the cleaned Kapton pieces were incubated for 10 min in a PAA aqueous solution (10 mg/ml. pH adjusted to 5.1 with NaOH) containing 0.5 M NaCl followed by rinsing three times with a 0.5 M NaCl aqueous solution. The Kapton pieces were then incubated for 10 min in a PEI aqueous solution (10 mg/ml. pH adjusted to 2.5 with HCl) containing 0.5 M NaCl followed by rinsing three times with a 0.5 M NaCl aqueous solution. Such a cycle was repeated to deposit the desired number of PEM layers on the Kapton pieces. To automate the deposition process, a peristaltic pump was used to deliver each of the polyelectrolyte solutions and the 0.5 M NaCl rinse solution to the sample chamber of the system. A two-way drain valve was used to remove the polyelectrolyte or the rinse solution to a waste chamber after a given incubation or rinsing step had been completed. A properly programmed microprocessor was used to operate the peristaltic pumps and the drain valve. After the desired number of deposition cycles has been finished, the resulting Kapton films were rinsed with DI water and dried in air at 60°C for 2 hours.

4.2. Contact angle measurements

Contact angle measurements were conducted (on a Rame-Hart goniometer equipped with a CCD camera (Rame-Hart Instrument Co., Succasunna, NJ, USA)) to evaluate the wetting of water, organic solvents, and inkjet inks on surface unmodified and PEM-modified Kapton HN films. **Table 1** shows that water and the water-based GO ink (which contained 60 wt% of glycerol for viscosity adjustment) exhibited an average contact angle of 76.6° and 72.4°, respectively, on a surface unmodified Kapton HN film. Organic solvents (ethanol and DMF), on the other hand, had quite small contact angles (<13°) on the same film. The commercial ethanol-based silver ink, with the presence of additional components such as a binder and a stabilizer, exhibited an average contact angle of 25.2° which was slightly higher than those of the two organic solvents. After PEM deposition on the Kapton HN film, the contact angles of both water and the water-based GO ink were significantly and reproducibly reduced. The

	Unmodified Kapton	Kapton with 1 PEM layer	Kapton with 3 PEM layers	Kapton with 4 PEM layers
Water	76.6 ± 3.9	41.0 ± 2.4	39.8 ± 1.9	37.4 ± 1.2
Ethanol	10.4 ± 2.5	12.1 ± 1.4	10.4 ± 1.9	12.2 ± 4.8
DMF	11.5 ± 1.3	12.5 ± 1.5	12.9 ± 0.1	13.3 ± 2.6
Water-based GO ink	72.4 ± 3.5	55.5 ± 2.6	53.7 ± 1.9	51.5 ± 1.2
ethanediol-based silver ink	25.2 ± 1.8	23.6 ± 0.3	24.1 ± 1.1	26.4 ± 1.6

Table 1. Contact angles of different solvents/inks on surface unmodified and PEM-modified Kapton HN films [1] (with permission from the Royal Society of Chemistry).

average contact angles of water and the water-based GO ink were reduced to 41.0° and 55.5°, respectively, after the deposition of only one layer of PEM, whereas the contact angles of the organic solvents (DMF and ethanol) and the ethanediol-based silver ink were essentially not changed (**Table 1**). It has been shown that the wetting of fluids onto sequentially adsorbed PEM layers was affected primarily by the outermost layer [39, 40]. In agreement with this previous observation, when additional PEM layers were deposited on the Kapton film, all the inks and the solvents examined in this work (water-based GO ink, ethanediol-based silver ink, DMF, ethanol, and water) exhibited little further changes in their contact angles (**Table 1**).

4.3. Printability assessment

Two organic solvent-based inks (a commercial ethanediol-based silver nanoparticle ink (Sun Chemical Corporation, Parsippany, NJ, USA) and a cyclohexanone/terpineol-based graphene ink (home-formulated based on the procedures described by Secor *et al.* [35])) and a water-based GO ink were examined for their inkjet printability on Kapton HN films before and after the PEM-based surface modification.

Figures 7 and **8** show high-resolution scanned images of silver IDE patterns and graphene patches, respectively, that were inkjet-printed on surface unmodified Kapton HN and Kapton HN which had been deposited with 1, 3 and 4 layers of PEMs. All of the silver IDEs and graphene patches exhibited uniform morphologies and precisely controlled shapes with sharp edges, as designed, irrespective of whether they had been printed on surface unmodified or PEM-modified Kapton HN films.

Figure 9a shows a square that was printed (five passes) with the GO ink on a surface unmodified Kapton KN film. The ink drops balled up to form isolated small "islands." On the other hand, after 1, 3, or 4 PEM layers had been deposited on a Kapton HN film, precisely controlled ink squares with sharp edges were able to be printed as designed. A typical GO ink square printed on a Kapton HN film that had been deposited with 4 PEM layers is shown in **Figure 9b**.

For electrically charged ink particles, similar to the bio-enabled method described above, this PEM-based surface modification method can also enhance the uniformity of the inkjet-printed thin films (by reducing the "coffee ring effect" during drying) compared with traditional Kapton surface modification methods.

4.4. Adhesion sustainability tests after chemical functionalization

For sensing applications, GO films normally need to be surface functionalized for the purpose of sensitivity and/or selectivity enhancement. Such surface functionalization includes reduction/oxidation and introduction and/or amplification of particular surface chemical groups

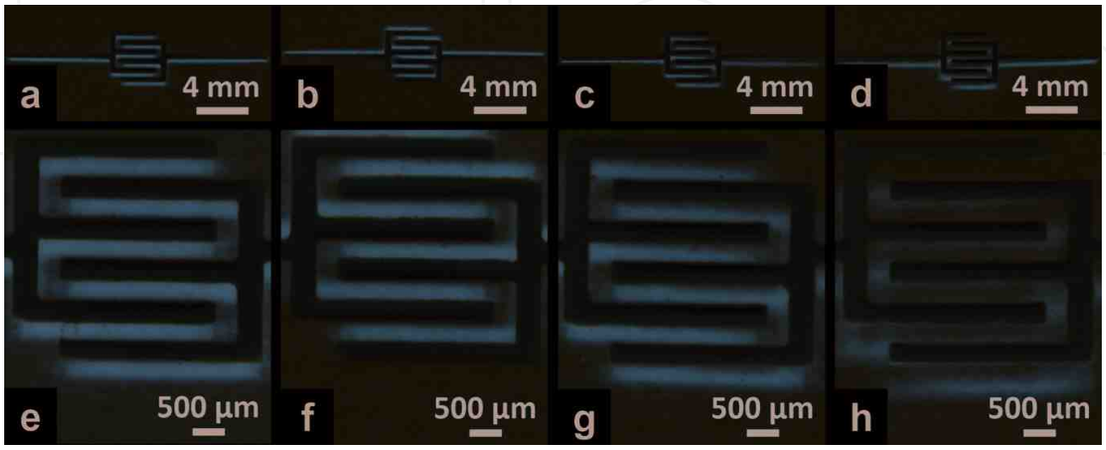

Figure 7. Scanned high-resolution images of silver IDE patterns printed on surface unmodified and PEM-modified Kapton HN films with a commercial ethanediol-based silver nanoparticle ink. (a), (b), (c) and (d) are low magnification images of silver IDEs inkjet-printed on surface unmodified, 1-PEM-layer-modified, 3-PEM-layer-modified and 4-PEM-layer-modified Kapton HN films, respectively. (e), (f), (g) and (h) are the high magnification counterparts of (a), (b), (c) and (d), respectively. All these silver IDE patterns were fabricated by inkjet-printing for 5 passes the silver ink on the appropriate Kapton films followed by drying at 120°C for 3 hours [1] (with permission from the Royal Society of Chemistry).

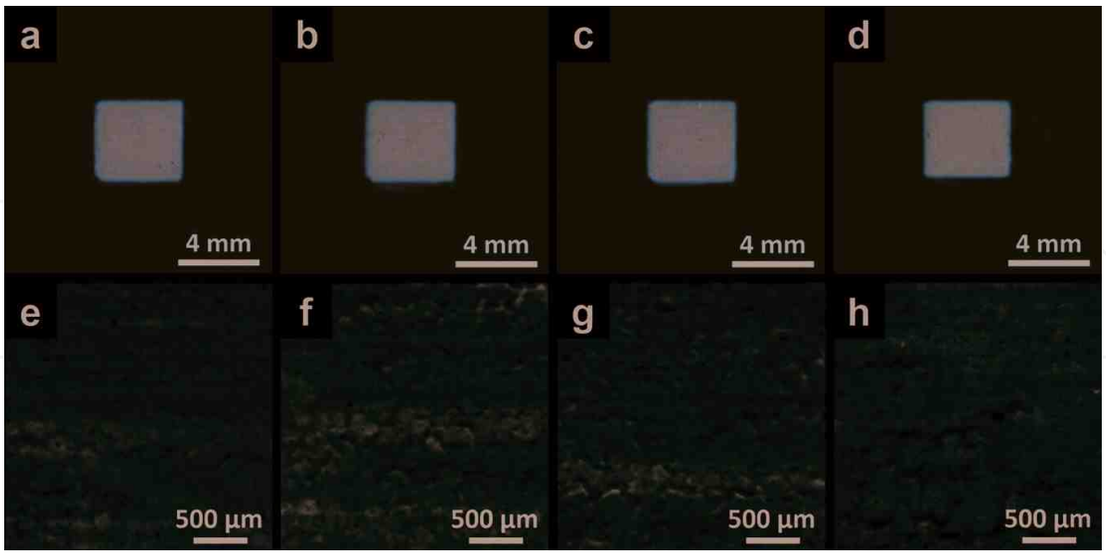

Figure 8. Scanned high-resolution images of graphene patches printed on surface unmodified and PEM-modified Kapton HN films with a cyclohexanone/terpineol-based graphene ink. (a), (b), (c) and (d) are low magnification images of graphene patches inkjet-printed on surface unmodified, 1-PEM-layer-modified, 3-PEM-layer-modified and 4-PEM-layer-modified Kapton HN films, respectively. (e), (f), (g), and (h) are the high magnification counterparts of (a), (b), (c), and (d), respectively. All these graphene patches were fabricated by inkjet-printing for 5 passes the graphene ink on the appropriate Kapton films followed by drying at 100°C for 1 hour [1] (with permission from the Royal Society of Chemistry).

and so on. The adhesion between the inkjet-printed GO films and the substrates has to be strong enough to survive such chemical functionalization.

To assess the adhesion of inkjet-printed rGO-based flexible sensors on Kapton HN substrates after such chemical functionalization, Kapton HN films were first surface modified via three approaches: UV/ozone treatment (traditional method), plasma treatment (traditional method), and the standard PEM-based deposition process described in this work. The UV/ozone treatment was conducted on a 95 mm x 95 mm Kapton HN film with a UVO Cleaner (Jelight Company Inc., Irvine, CA, USA) for 5 min. The plasma treatment was performed on a 95 mm x 95 mm Kapton HN film with a plasma cleaner (model PDC-001. Harrick Scientific Corp., Ossining, NY, USA) in air for 20 min with the RF power set to the "high" level. GO patches were then inkjet-printed on the resulting surface modified Kapton films with the water-based GO ink. The inkjet-printed GO traces were then fired in nitrogen for one hour to be reduced to their rGO counterparts, followed by chemical treatments to introduce various surface chemical functional groups (hexafluoroisopropyl, amine, acrylate, and hydroxyl groups) to the resulting rGO patches.

After the reduction or a GO film functionalization process, the adhesion between the rGO patches and the surface-modified Kapton substrates was evaluated by visual inspection while slowly bending (to a radius of curvature of ˜1 cm) the rGO-on-Kapton structure. The structures were first bent 150 times in tension and then another 150 times in compression. **Table 2** summarizes the results of such adhesion sustainability bend tests. The GO films inkjet-printed on all the surface-modified Kapton HN substrates remained attached to the substrates after the thermal reduction and such bending. After the thermal reduction followed by each of the film functionalization treatments, the GO films printed on the 3-PEM-layer-modified or 4-PEM-layer-modified Kapton HN film remained attached upon bending (**Table 2**). On the other hand, the adhesion of the inkjet-printed GO films on the UV/ozone-, plasma-treated, or 1-PEM-layer-modified Kapton HN substrates was not as universally robust after the thermal reduction followed by the various film functionalization treatments. As shown in **Table 2**, the adhesion sustainability of the inkjet-printed GO films increased with increasing number of PEM layers on the Kapton substrates, which is probably due to the following reasons: each time after a polyelectrolyte (PAA or PEI) had bound to a Kapton HN substrate surface or to the oppositely charged polyelectrolyte which had previously bound to the substrate, there still existed nonoccupied binding

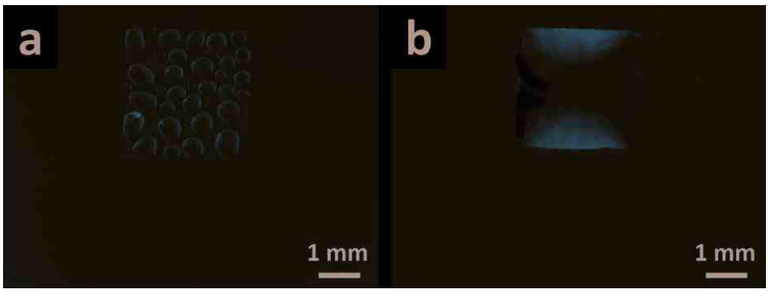

Figure 9. Optical images of GO squares printed (5 passes) with a water-based GO ink on surface unmodified (a) and 4-PEM-layer-modified (b) Kapton substrates [1] (with permission from the Royal Society of Chemistry).

sites (point charges) on the substrate surface [39]. One PEM layer deposited on the substrate would probably be able to cover most (but not all) of the blank Kapton HN surface, which allowed for reasonably good printability for the GO ink. As more PEM layers were deposited, the uncovered substrate surface gradually decreased and the surface positive charge density gradually increased. As a result, when the GO ink particles (negatively charged) were inkjet-printed on, and bound to, such surface modified substrate, the adhesion between the inkjet-printed GO film and the substrate gradually increased.

Modification to GO	**Modification to Kapton**				
	UV/ozone	**Plasma**	**1 PEM layer**	**3 PEM layers**	**4 PEM layers**
Thermal reduction	+	+	+	+	+
Hexafluoroisopropyl addition	—	—	+	+	+
Amine addition	—	—	+	+	+
Acrylate addition	NA	NA	—	+	+
Hydroxyl addition	NA	NA	NA	+	+

Table 2. Adhesion sustainability of GO films on surface-modified Kapton HN substrates upon thermal reduction followed by a number of surface group-introducing reactions ("+": the adhesion survived the corresponding chemical treatment; "—": the adhesion did not survive the corresponding chemical treatment; "NA": the corresponding chemical treatment was not performed since a prior step had peeled the GO film off from the substrate) [1] (with permission from the Royal Society of Chemistry).

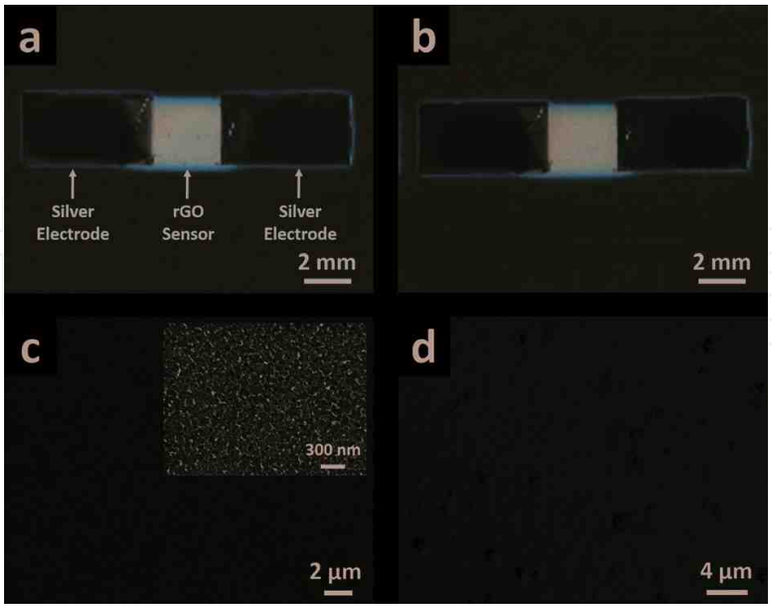

Figure 10. Morphological analyses of a single-layered rGO-based sensor printed on a 4-PEM-layer-modified Kapton HN substrate before and after the bend testing. The water-based GO ink and the ethanediol-based Ag ink were printed for 60 and 5 inkjet passes, respectively. (a) and (b) optical images of the sensor before and after the bend testing, respectively. (c) Low and high (inset) magnification SEM images of a silver IDE of the sensor after the bend testing. (d) SEM image of the rGO patch of the sensor after the bend testing [1] (with permission from the Royal Society of Chemistry).

4.5. Fabrication and bend testing of all-inkjet-printed flexible gas sensors

Single-layered, rGO-based gas sensors were fabricated on a 4-PEM-layer-modified Kapton HN substrate following the procedures described in Section 3.3. A such fabricated sensor, as shown in **Figure 10a**, was subjected to bend testing. The sensor was bent, to a radius of curvature of ~1 cm, 1000 times in tension followed by another 1000 times in compression. During the bending process, conductivity measurements were performed on the sensor after every 50 times of bending. The conductivity of the sensor was found to be virtually the same (i.e. a resistance of ~6 kΩ) throughout the whole bend testing as that before the bending. Optical and SEM microscopic analyses were conducted after such repeated bending to examine the morphology of the sensor. No apparent cracks on either the silver electrodes or the rGO patch were observed and the sensor remained the same morphology as that before the bending (**Figure 10b–d**).

5. Conclusions

The slip additive in Kapton HN films contains a significant amount of crystalline $CaCO_3$. Taking advantage of the electric charges borne by the additive particles at a neutral or acidic pH, two mild and environmentally friendly wet chemical approaches have been recently developed to surface modify Kapton HN films. The resulting surface modified films allowed for not only great printability of both water- and organic solvent-based inks (thus facilitating the full-inkjet-printing of entire flexible electronic devices) but also strong adhesion between the inkjet-printed traces and the substrate films. Different from the traditional Kapton surface modification approaches which target the surface polyimide matrix, these two mild methods targeted the electric charges borne by the additive particles.

The bio-enabled method, which utilized two clinical biomolecules and was conducted in aqueous salt solutions at a neutral pH, room temperature, and atmospheric pressure, was maximally mild and minimally destructive. The flexible rGO-based gas sensors fully inkjet-printed on the resulting surface modified Kapton HN films survived a Scotch-tape peel test and were found insensitive to repeated bending to a small 0.5 cm radius.

The computer-controlled PEM-based method involved the use of only weak polyelectrolytes (to enable systematic and simple control of the PEMs formed via adjustment of the pH of the polyelectrolyte solutions). The adhesion sustainability increased with increasing number of PEM layers. The rGO-based sensors printed on the resulting surface modified (with 4 layers of PEM layers) Kapton HN substrate was insensitive to repeated (1000 times in tension and another 1000 times in compression) bending to a radius of curvature of ~1 cm.

For electrically charged ink particles, both methods can enhance the uniformity of the inkjet-printed films via reduction of the "coffee ring effect" during drying.

The two methods have not only introduced new means to tune the surface properties of Kapton HN films thus allowing for the full-inkjet-printing of flexible and robust electronic devices but also brought forth solutions to significantly reduce of the environmental pollutions associated with inkjet-printing of Kapton-based flexible electronic devices.

Acknowledgements

We thank the financial support from the Defense Threat Reduction Agency (DTRA) (USA) via Award No. HDTRA1-09-14-FRCWMD/TA3.

Conflict of interest

The authors declare no conflict of interests.

Author details

Yunnan Fang[1]* and Manos M. Tentzeris[2]

*Address all correspondence to: yunnan.fang@mse.gatech.edu

1 School of Materials Science and Engineering, Georgia Institute of Technology, Atlanta, Georgia, USA

2 School of Electrical and Computer Engineering, Georgia Institute of Technology, Atlanta, Georgia, USA

References

[1] Fang YN, Hester JGD, deGlee BM, Tuan CC, Brooke PD, Le TR, et al. A novel, facile, layer-by-layer substrate surface modification for the fabrication of all-inkjet-printed flexible electronic devices on Kapton. Journal of Materials Chemistry C. 2016;**4**(29):7052-7060. DOI: 10.1039/c6tc01066k

[2] Fang YN, Hester JGD, Su WJ, Chow JH, Sitaraman SK, Tentzeris MM. A bio-enabled maximally mild layer-by-layer Kapton surface modification approach for the fabrication of all-inkjet-printed flexible electronic devices. Scientific Reports. 2016;**6**:39909. DOI: 10.1038/srep39909

[3] Gouzman I, Girshevitz O, Grossman E, Eliaz N, Sukenik CN. Thin film oxide barrier layers: Protection of Kapton from space environment by liquid phase deposition of titanium oxide. ACS Applied Materials & Interfaces. 2010;**2**(7):1835-1843. DOI: 10.1021/am100113t

[4] Inagaki N, Tasaka S, Hibi K. Surface modification of Kapton film by plasma treatments. Journal of Polymer Science Part A: Polymer Chemistry. 1992;**30**(7):1425-1431. DOI: 10.1002/pola.1992.080300722

[5] Bachman BJ, Vasile MJ. Ion-bombardment of polyimide films. Journal of Vacuum Science & Technology A: Vacuum, Surfaces, and Films. 1989;**7**(4):2709-2716. DOI: 10.1116/1.575779

[6] Shin JW, Jeun JP, Kang PH. Surface modification and characterization of N+ ion implantation on polyimide film. Macromolecular Research. 2010;**18**(3):227-232. DOI: 10.1007/s13233-010-0310-x

[7] Le TR, Lakafosis V, Lin ZY, Wong CP, Tentzeris MM. Inkjet-printed graphene-based wireless gas sensor modules. In: 2012 IEEE 62nd Electronic Components and Technology Conference (ECTC). San Diego, CA, USA: IEEE; 2012

[8] Ghosh I, Konar J, Bhowmick AK. Surface properties of chemically modified polyimide films. Journal of Adhesion Science and Technology. 1997;**11**(6):877-893. DOI: 10.1163/156856197x00967

[9] Huang XD, Bhangale SM, Moran PM, Yakovlev NL, Pan JS. Surface modification studies of Kapton (R) HN polyimide films. Polymer International. 2003;**52**(7):1064-1069. DOI: 10.1002/pi.1143

[10] Thomas RR, Buchwalter SL, Buchwalter LP, Chao TH. Organic-chemistry on a polyimide surface. Macromolecules. 1992;**25**(18):4559-4568. DOI: 10.1021/ma00044a016

[11] Least BT, Willis DA. Modification of polyimide wetting properties by laser ablated conical microstructures. Applied Surface Science. 2013;**273**:1-11. DOI: 10.1016/j.apsusc.2012.12.141

[12] Gallais L, Bergeret E, Wang B, Guerin M, Benevent E. Ultrafast laser ablation of metal films on flexible substrates. Applied Physics A: Materials Science & Processing. 2014;**115**(1):177-188. DOI: 10.1007/s00339-013-7901-2

[13] Ghosh MK, Mittal KL. Polyimides: Fundamentals and Applications. New York, USA: Marcel Dekker; 1996

[14] Williams MK, Smith AE, Huelskamp MA, Armstrong KP, Brandon JL, Lavoie JM. Kapton HN investigations. MOUND. 1990 September;**28**:1990

[15] Zhou LS, Wanga A, Wu SC, Sun J, Park S, Jackson TN. All-organic active matrix flexible display. Applied Physics Letters. 2006;**88**(8). DOI: 10.1063/1.2178213

[16] Ota I, Ohnishi J, Yoshiyam M. Electrophoretic image display (EPID) panel. Proceedings of the IEEE. 1973;**61**(7):832-836. DOI: 10.1109/proc.1973.9173

[17] Gelinck GH, Huitema HEA, Van Veenendaal E, Cantatore E, Schrijnemakers L, Van der Putten J, et al. Flexible active-matrix displays and shift registers based on solution-processed organic transistors. Nature Materials. 2004;**3**(2):106-110. DOI: 10.1038/nmat1061

[18] Granqvist CG. Transparent conductors as solar energy materials: A panoramic review. Solar Energy Materials and Solar Cells. 2007;**91**(17):1529-1598. DOI: 10.1016/j.solmat.2007.04.031

[19] Yoon J, Baca AJ, Park SI, Elvikis P, Geddes JB, Li LF, et al. Ultrathin silicon solar microcells for semitransparent, mechanically flexible and microconcentrator module designs. Nature Materials. 2008;**7**(11):907-915. DOI: 10.1038/nmat2287

[20] Sekitani T, Yokota T, Zschieschang U, Klauk H, Bauer S, Takeuchi K, et al. Organic nonvolatile memory transistors for flexible sensor arrays. Science. 2009;**326**(5959):1516-1519. DOI: 10.1126/science.1179963

[21] Le TR, Lakafosis V, Tentzeris MM, Lin ZY, Fang YN, Sandhage KH, et al. Novel techniques for performance enhancement of inkjet-printed graphene-based thin films for wireless sensing platforms. In: 2013 European Microwave Conference (EuMC); October 6-11 2013; Nuremberg. Germany: IEEE; 2013. pp. 17-20

[22] Shi JD, Li XM, Cheng HY, Liu ZJ, Zhao LY, Yang TT, et al. Graphene reinforced carbon nanotube networks for wearable strain sensors. Advanced Functional Materials. 2016;**26**(13):2078-2084. DOI: 10.1002/adfm.201504804

[23] Fang YN, Akbari M, Sydanheimo L, Ukkonen L, Tentzeris MM. Sensitivity enhancement of flexible gas sensors via conversion of inkjet-printed silver electrodes into porous gold counterparts. Scientific Reports. 2017;**7**. DOI: 10.1038/s41598-017-09174-5

[24] Han TH, Lee Y, Choi MR, Woo SH, Bae SH, Hong BH, et al. Extremely efficient flexible organic light-emitting diodes with modified graphene anode. Nature Photonics. 2012;**6**(2):105-110. DOI: 10.1038/nphoton.2011.318

[25] Schmied B, Gunther J, Klatt C, Kober H, Raemaekers E. STELLA—STretchable ELectronics for large area applications-a new technology for smart textiles. In: Vincenzini P, Paradiso R, editors. Smart Textiles. Advances in Science and Technology. Vol. 60. Stafa-Zurich, Switzerland: Trans Tech Publications Ltd; 2009. pp. 67-73

[26] Myny K, Steudel S, Vicca P, Beenhakkers MJ, van Aerle N, Gelinck GH, et al. Plastic circuits and tags for 13.56 MHz radio-frequency communication. Solid-State Electronics. 2009;**53**(12):1220-1226. DOI: 10.1016/j.sse.2009.10.010

[27] Chen MX. Printed electrochemical devices using conducting polymers as active materials on flexible substrates. Proceedings of the IEEE. 2005;**93**(7):1339-1347. DOI: 10.1109/jproc.2005.851532

[28] Wang PS, Wittberg TN, Wolf JD. A characterization of Kapton polyimide by X-ray photoelectron-spectroscopy and energy dispersive spectroscopy. Journal of Materials Science. 1988;**23**(11):3987-3991. DOI: 10.1007/bf01106825

[29] Hin TY. Materials and processes to enable polymeric waveguide integration on flexible substrates [thesis]. Loughborough: Loughborough University; 2009

[30] McClure DJ. Polyimide film as a vacuum coating substrate. In: Annual Technical Conference Proceedings - Society of Vacuum Coaters; 2010. 53rd ed. pp. 608-12

[31] Halikia I, Zoumpoulakis L, Christodoulou E, Prattis D. Kinetic study of the thermal decomposition of calcium carbonate by isothermal methods of analysis. European Journal of Mineral Processing and Environmental Protection. 2001;**1**(2):89-102

[32] Somasundaran P, Agar GE. The zero point of charge of calcite. Journal of Colloid and Interface Science. 1967;**24**:433-440

[33] Rossmann P, Matousovic K, Horacek V. Protamine-heparin aggregates-their fine-structure, histochemistry, and renal deposition. Virchows Archiv B-Cell Pathology Including Molecular Pathology. 1982;**40**(1):81-98. DOI: 10.1007/bf02932853

[34] Constable S, Winstanley P, Walley T. Medical Pharmacology: A Clinical Core Text for Integrated Curricula with Self Assessment. 3rd ed. Elsevier Limited; 2007

[35] Secor EB, Prabhumirashi PL, Puntambekar K, Geier ML, Hersam MC. Inkjet printing of high conductivity, flexible graphene patterns. Journal of Physical Chemistry Letters. 2013;**4**(8):1347-1351. DOI: 10.1021/jz400644c

[36] Rye RR, Ricco AJ. Patterned adhesion of electrolessly deposited copper on poly(tetrafluoroethylene). Journal of the Electrochemical Society. 1993;**140**(6):1763-1768. DOI: 10.1149/1.2221638

[37] Sener U. Adhesion of Copper to UV Photo-Oxidized Kapton and Upilex-S Polyimide Surfaces [Thesis]. Rochester, NY: Rochester Institute of Technology; 2004

[38] Yoo D, Shiratori SS, Rubner MF. Controlling bilayer composition and surface wettability of sequentially adsorbed multilayers of weak polyelectrolytes. Macromolecules. 1998;**31**(13):4309-4318. DOI: 10.1021/ma9800360

[39] Lowack K, Helm CA. Molecular mechanisms controlling the self-assembly process of polyelectrolyte multilayers. Macromolecules. 1998;**31**(3):823-833. DOI: 10.1021/ma9614454

[40] Amarnath CA, Hong CE, Kim NH, Ku BC, Kuila T, Lee JH. Efficient synthesis of graphene sheets using pyrrole as a reducing agent. Carbon. 2011;**49**(11):3497-3502. DOI: 10.1016/j.carbon.2011.04.048

IntechOpen